IAA-AAS-DyCoSS2-14-16-03

EVALUATING ORBITS WITH POTENTIAL TO USE SOLAR SAIL FOR STATION-KEEPING MANEUVERS

Thais C. Oliveira,[*] and Antonio F. B. A. Prado[†]

The purpose of this paper is to find the necessary and the sufficient conditions to use solar sails in order to compensate or to reduce the perturbation effects due to external forces received by a satellite. The study considers a satellite with the following disturbing forces: the solar radiation pressure, the zonal harmonic perturbation J_2 to J_4 and the third body perturbation due to the Sun and the Moon. The necessary and the sufficient conditions are, for a given orbit, the area and the attitude that the solar sail must have in order to compensate or to reduce the effects of the other perturbation forces. In this way, the cost of the station keeping maneuver can be reduced in terms of the fuel consumption, since there is less perturbation acting on the satellite. Consequently, the lifetime of the satellite can be extended, since it is dependent from the fuel left to perform orbital maneuvers. The use of the integrals over the time is a new approach that provides the accumulated effects of the perturbation forces. In this way, it is also possible to evaluate the magnitude of each perturbation force acting separately or all added together and also the evaluation of the magnitude of the reduction of the disturbing forces with the solar sail usage. The result of this integral is also the total velocity variation that the satellite suffers from the perturbation forces. In addition, the evaluation of the direction of the perturbation forces can guarantee the use of the solar sail to reduce the shifts caused by the external forces acting on the satellite by applying a disturbing force from the solar sail in the opposite direction of the other perturbations.

INTRODUCTION

This paper aims to find the optimal direction and the value of the projected area illuminated by the Sun that a solar sail must have in order to use the solar radiation pressure as a disturbing force that reduces or eliminate the other perturbation forces. The perturbation forces considered are: solar radiation pressure, third body perturbation of the Sun and the Moon and the J_n perturbation from J_2 to J_4. The idea is to use a propulsion system to compensate the perturbations that the solar radiation pressure is not able to do, in order to keep the orbit of the spacecraft keplerian all the time. This approach is used in order to map orbits that have a good potential to use this concept and not to estimate the fuel consumption to realize those maneuvers, because the exact fuel required depends on the control strategy used and the constraints of the mission.

[*] National Institute for Space Research (INPE), Space Engineering Technology, Space Mechanics and Control, thais.tata@gmail.com
[†] National Institute for Space Research (INPE), Space Engineering Technology, Space Mechanics and Control, prado@dem.inpe.br

For the optimal solution of the solar sail, it is considered that the size of the solar sail can vary along the orbit. Although the solution might look not practical, since it is very hard to build solar sail that can vary its size, it can be convenient for a first analysis of the mission to guarantee that the magnitude of the disturbing forces has the same magnitude provided by the solar sail.

Also, two sub-optimal analyses are considered: one is obtained by choosing a fixed area of the solar sail and the other one is obtained using a fixed area for the solar sail and some limitations on the degrees of freedom for the solar sail attitude. The time integral of the magnitude of the disturbing forces is a technique used is this paper to guarantee that the use of the solar sail is valid and to reduce the other perturbation forces along the orbit.[1,2,3]

The Solar Radiation Pressure

The solar radiation pressure is one of the perturbation forces that act on the satellite, deviating the orbit of the spacecraft to a non-Keplerian orbit. The solar radiation pressure occurs when the radiation emitted by the Sun collides with the surface of the satellite, resulting in a force acting on that surface. The solar radiation pressure can not only change the orbital motion of the satellite, but it can also change the attitude of the satellite, if the solar radiation pressure force is not directed to the center of mass of the satellite.[4]

Although the solar radiation pressure is a disturbing force, there are some cases where it can be used for the attitude control to help the maintenance of the orientation of the satellite[5] or even for orbital maintenance.[6,7,8,12]

This paper is concerned with the use of the solar radiation pressure in order to reduce the shifts caused by the other perturbation forces. The solar sail is used here to expand the effects of the solar radiation pressure and to create a perturbation in the opposite direction of the other disturbing forces. To achieve this purpose, the attitude of the solar sail is an important key to guarantee that the disturbing forces of the solar sail and the external forces acting on the satellite are opposite.

The magnitude of the solar radiation pressure acceleration applied to a spacecraft or a solar sail is given by:[9]

$$a_{solar} = \gamma(1+r)P_s\frac{A_s}{m}cos^2\emptyset\hat{f} \tag{1}$$

where r is the reflectivity of the surface, assuming values from 0 to 1; P_s is the ratio of the solar constant, 1360 W/m^2 at one A.U., to the speed of the light; A_s is the projected area of the satellite or the solar sail that is illuminated by the Sun; m is mass of the satellite; $\emptyset$ is the angle between the direction of the light flux and the normal of the satellite and γ determines the Earth's shadow region. The unit vector $\hat{f}$ represents the direction of the force applied to the surface of the body and it is given by:[10]

$$\hat{f} = -\frac{(1-r)\hat{\sigma}+2rcos\emptyset\hat{n}}{\sqrt{(1-r)^2+4rcos^2\emptyset}} \tag{2}$$

where $\hat{\sigma}$ is the unit vector with the opposite direction to the light flux and $\hat{n}$ is the unit vector pointing to the normal of the surface.

Figure 1 shows the light interaction with a smooth surface of the body with the unit vectors $\hat{\sigma}$, $\hat{n}$, $\hat{f}$ and the angles δ and $\emptyset$.[10]

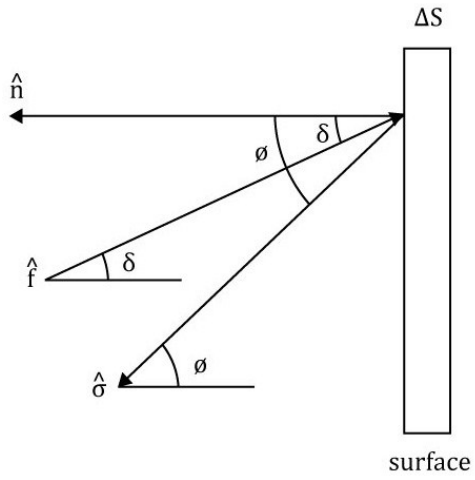

Figure 1. The light interaction with a smooth surface.

The angle δ provides the direction of the solar radiation pressure force and it is the angle between the unit vectors $\hat{n}$ and $-\hat{f}$. In the way shown in Eq. (2) and Figure 1, the direction of the force caused by the solar radiation pressure is related to the reflectivity of the surface r and the angle between the direction of the light flux $\emptyset$ with the normal of the surface. If the value of the reflectivity of the surface is different from one, some of the energy of the light flux is absorbed by the surface and then the direction of the solar radiation force is not the opposite to the normal unit vector $\hat{n}$. Nevertheless, if the angle $\emptyset$ is zero, then, even though the coefficient of reflectivity might be different from one, the direction of the solar radiation pressure force is opposite to the normal unit vector.

The shadow regions given by γ is determined by conical projections of the umbra and penumbra shadows, given the position and the shape of the Earth, the Sun and the distance between those celestial bodies.[11] The coefficient $\gamma = 1$ occurs when the satellite is in the illuminated region. If $\gamma = 0.5$, then the satellite is located at the penumbra region and, if $\gamma = 0$, it is at the umbra region. A schematic figure illustrating this configuration is given in Figure 2.[11]

For practical reasons, since this paper is concerned with a conceptual design and analysis of spacecraft's orbits, the shape of the satellite was considered to be very simple. The satellite has a square shape with area of 4 m^2 for each side. The surface of the satellite is smooth and the reflectivity parameter r is considered to be 0.8. For the attitude of the satellite, it is considered that one of the sides is always pointing to the center of the Earth.

For the solar sail, the shape considered was a smooth surface with negligible base area Δs, as shown in Figure 1. Once the solar sail has a smooth surface, there is no need to define the shape of the solar sail surface. It is only necessary to define the area of the smooth surface A_s and the normal unit vector of the solar sail for its attitude. The reflectivity parameter of the solar sail was considered to be $r = 0.9$. This value is realistic although it is not the ideal one, that should have 100% of reflectivity.[12]

The solar sail is used to compensate the other perturbation forces that deviates the orbit of the satellite. Therefore, it is considered that the satellite is able to change the attitude of the solar sail at every instant of time, compensating the torques and other perturbations that the attitude motion suffers and also to change the area A_s to the optimal case.

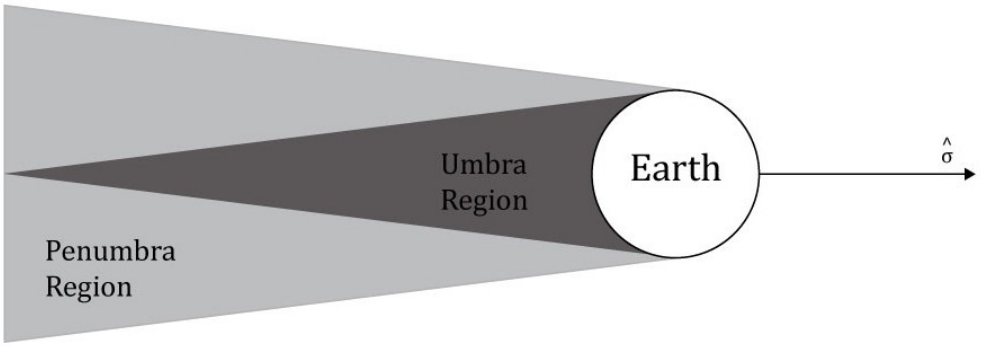

Figure 2. The illustration of the umbra, penumbra and illuminated areas.

The first sub-optimal case considers that the area A_s is fixed, but the attitude of the solar sail is optimal. The second sub-optimal case considers that the solar sail attitude has some constraints in the degrees of freedom.

For the constrained solar sail attitude, it is important to explain the reference system fixed on the satellite, in order to have a better understanding of the attitude constraint. The non-inertial reference system fixed in the satellite has the x axis in the radial direction directed to the centre of the Earth, the y axis is perpendicular to the x axis and it lies in the orbital plane; and the z axis is normal to the orbital plane and its direction is given by the cross product of the x and y axes. The solar sail can rotate freely on the y axis, but for the rotation of the z axis, the solar sail can only rotate from -30 to 30 degrees. The rotation on the x axis does not matter for this geometry, since it does not influence the results obtained. Figure 3 is the geometric illustration for the restricted degrees of freedom for the second sub-optimal case.

As shown in Figure 3, one of the sides of the satellite is always pointing to the radial direction $\hat{r}$ or to the x axis of the reference frame of the satellite. This attitude of the satellite is also considered for the optimal and the first sub-optimal case. It is assumed that the satellite is capable of controlling the attitude of the satellite at every instant of time and that its attitude is given by the normal vector $\hat{n}$ (see Figure 1).

Nevertheless, there are some parts of the orbit where the solar radiation pressure cannot control the other perturbation forces, whether because the satellite is on the shadow of the Earth or because the optimal angle of the incidence of the flux of the Sun radiation $\emptyset$ is larger than $\pi/2$ rad. Whenever the solar radiation cannot control the other perturbation forces, the solar sail becomes inactive by rotating the panels and creating a perpendicular direction of the normal of the surface of the solar sail with the direction of the light flux. In this way, the light flux collides with the neglected base area of the solar sail and it becomes inactive.

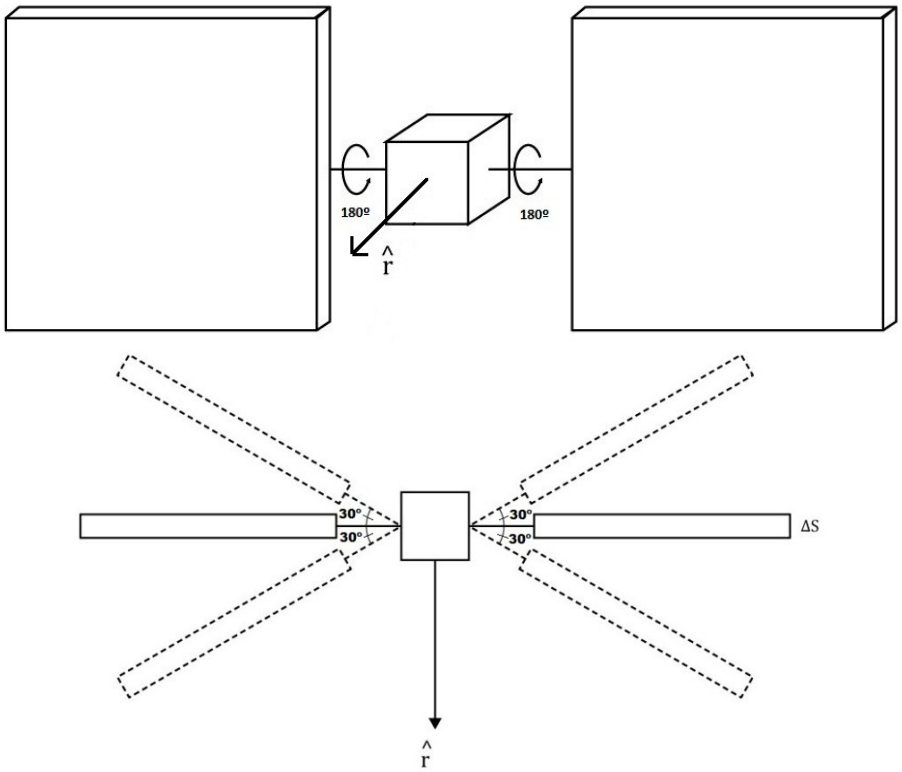

Figure 3. The degrees of freedom for the second case of the sub-optimal approach.

Note that all the computations and results are performed and presented in a inertial coordinate system known as the "vernal coordinate system," where the X axis is pointed to the vernal point and the centre of the Earth is the origin of the coordinate system.

The Third Body Perturbation

The third-body perturbation in this paper includes the perturbations of the Sun and the Moon. The position of the Sun and the Moon are given by the ephemeris models presented in several references.[13,14,15] The potential of the gravitational force due to the Sun and the Moon is given by Equation (3): [1,2]

$$U = -G\left[m_M\left(\frac{xx_M+yy_M+zz_M}{r_{EM}^3}-\frac{1}{r_M}\right)+m_S\left(\frac{xx_S+yy_S+zz_S}{r_{ES}^3}-\frac{1}{r_S}\right)\right] \tag{3}$$

where the coordinates of the Sun are x_s, y_s and z_s; the coordinates of the Moon are x_m, y_m and z_m; the coordinates of the spacecraft are x, y and z; G is the gravitational constant; m_S is the mass of the Sun; m_M is the mass of the Moon and r_{EM}, r_{ES}, r_M and r_S are the distances from the Moon to the Earth; from the Sun to the Earth; from the spacecraft to the Moon and from the spacecraft to the Sun, respectively. The reference system considered in this paper is the inertial one with the X axis pointed to the vernal point, the XY plane is the equatorial plane of the Earth and the centre of the reference system is the Earth.

Concerning the disturbing force of the third body, the gradient of the potential, that gives the perturbing force, is given by:

$$\nabla U = f_x + f_y + f_z \tag{4}$$

where f_x, f_y and f_z are:[1,16]

$$f_x = -G\left(m_M\left(\frac{x_M}{{r_{EM}}^3} - \frac{x_M - x}{{r_M}^3}\right) + m_S\left(\frac{x_S}{{r_{ES}}^3} - \frac{x_S - x}{{r_S}^3}\right)\right) \tag{5}$$

$$f_x = -G\left(m_M\left(\frac{y_M}{{r_{EM}}^3} - \frac{y_M - y}{{r_M}^3}\right) + m_S\left(\frac{y_S}{{r_{ES}}^3} - \frac{y_S - y}{{r_S}^3}\right)\right) \tag{6}$$

$$f_z = -G\left(m_M\left(\frac{z_M}{{r_{EM}}^3} - \frac{z_M - z}{{r_M}^3}\right) + m_S\left(\frac{z_S}{{r_{ES}}^3} - \frac{z_S - z}{{r_S}^3}\right)\right) \tag{7}$$

The J_2, J_3 and J_4 Perturbations

The Earth is not perfectly symmetric and it does not have a homogeneous distribution of mass. This non-symmetry and this mass displacement can be considered as a disturbing force that acts on the satellite. The oblatness of the Earth has the greatest influence on this disturbing force and it is usually described with the help of the J_2 coefficient of the zonal harmonic. This paper considers the J_2 to J_4 coefficients as the disturbing forces related to the non-symmetry of the Earth. The J_2, J_3 and J_4 are dimensionless constants and their values considered here are $J_2 = 1.08263 \times 10^{-3}$, $J_3 = -2.54 \times 10^{-6}$ and $J_4 = -1.61 \times 10^{-6}$.[17] Before describing the gravitational potential and the disturbing force due to the non-spherical Earth, it is necessary to define the position vector used in this paper and it is given by Equation (8):[17]

$$\mathbf{r} = r\boldsymbol{i_r} + r\Theta\boldsymbol{i_\theta} \tag{8}$$

where the unit vector i_r denotes the radial direction and the unit vector i_θ denotes the southward direction in the local horizontal frame. The angle Θ is actually the co-latitude of the position of the sub-satellite point. This angle is determined in this paper by the initial parameter of the initial time, date and year of the begging of the simulation.

Subsequently, the gravitational potential of the perturbation of this paper is described with the help of the position vector, as follows:[17]

$$U(r, \emptyset) = -\frac{GM_0}{r}\left\{\sum_{n=2}^{4}\left(\frac{Re}{r}\right)^n J_n P_n(\cos\Theta)\right\} \tag{9}$$

where Re is the equatorial radius of the Earth, M_0 is the mass of the Earth, P_n is the Legendre polynomial of n^{th}degree, J_n is the spherical harmonic coefficient of n^{th} degree.

The gravity is a conservative force, therefore it can be expressed by the gradient of the potential given in Equation (9). This gradient in Equation (10), with respect to the position vector in Equation (8), is:[17]

$$\mathbf{g} = g_r\boldsymbol{i_r} + g_\emptyset\boldsymbol{i_\emptyset} \tag{10}$$

where

$$g_r = -\frac{GM}{r^2}\left[-3J_2\left(\frac{Re}{r}\right)^2 P_2(\cos\emptyset) - 4J_3\left(\frac{Re}{r}\right)^3 P_3(\cos\emptyset) - 5J_4\left(\frac{Re}{r}\right)^4 P_4(\cos\emptyset)\right] \tag{11}$$

and

$$g_{\emptyset} = \frac{3GM}{r^2}\left(\frac{Re}{r}\right)^2 \sin\emptyset\cos\emptyset\left[J_2 + \frac{1}{2}J_3\left(\frac{Re}{r}\right)\sec\emptyset\,(5\cos^2\emptyset - 1) + \frac{5}{6}J_4\left(\frac{Re}{r}\right)^2(7\cos^2\emptyset - 3)\right] \quad (12)$$

The Integral Approach

The integral approach is based on the integral of the magnitude of the disturbing forces along the orbit for one orbital period. This integral is called PI in this paper and it is given by Equation (13):[1]

$$PI = \int_0^T |F|\,dt \quad (13)$$

where F is the disturbing force or forces per unit of mass of the satellite, t is the time and T is the period of the orbit.

The integral approach, given by Equation (13), considers a Keplerian orbit for the satellite, even though there are disturbing forces acting on the satellite. Therefore, it is assumed that the variations of the orbital elements during one orbital period, the time of integration, is not too large. At first glance, this approach is not practical, since the fuel consumption for this type of station-keeping maneuver can be very demanding. Nevertheless, this approach can be useful to map orbits that are less perturbed and so have a good potential for requiring less fuel for station-keeping, independent of the constraints imposed and the control strategy adopted. The PI value indicates the velocity change that the satellite suffers from the disturbing forces and this value is also associated with the deviation of the Keplerian elements of the orbit. [19]

In this way, the integral approach is used to test the optimal and sub-optimal solutions of the solar sail used to analyze the magnitude of the disturbing forces with and without the solar sail for a complete orbit of the satellite.

RESULTS

The results of this paper are based on the geostationary orbit. The initial parameters used are given in Table 1. The initial Keplerian elements of the orbit are: semi-major axis = 42164000 m; eccentricity = 0; inclination = 0°; argument of perigee = 0°; right ascension of the ascending node = 0°; true anomaly = 0°.

Table 1. Initial parameters for the solar radiation pressure

Reflectivity of the satellite	0.8
Area of the square side of the satellite (m^2)	4
Reflectivity of the solar sail	0.9
Maximum area of the solar sail (for the optimal case) (m^2)	500

The Optimal Case

The first analysis for the optimal case begins the simulation in January 01, 2014 at 5:30 GMT. The results are shown in Figures 4 to 6.

Figure 4 shows the magnitude of the acceleration of the disturbing forces as a function of the eccentric anomaly of the spacecraft. The blue line is the magnitude of the perturbation that acts on the satellite and the red one represents the magnitude of the solar sail. From the eccentric

anomaly 70 to 140 degrees, approximately, the magnitude of the solar sail perturbation is the same as all perturbations, therefore, for this range, the solar sail can compensate fully the other perturbation forces. Nevertheless, for different values of the eccentric anomaly of the spacecraft, the solar sail magnitude force is not able to compensate the other perturbation forces fully, it is just able to reduce their effects. For these initial parameters of the simulation, the satellite is always illuminated by the Sun. Figure 5 shows the incident angle Ø as a function of the eccentric anomaly. According to Equation 1, the magnitude of the solar sail force is related to this incidence angle, and, as this incidence angle approaches zero, the magnitude of the solar radiation pressure increases and it decreases when the angle of incidence increases.

The optimal case considers a variable area for the solar sail with the maximum value of 500 m^2, as shown in Figure 6. Using Figures 4, 5 and 6, it is clear that, as the incident angle decreases, the value of the area of the solar sail required to compensate the other perturbations decrease, since the magnitude of the solar sail is related to the incident angle. Nevertheless, the incident angle also determines the direction of the perturbation of the solar sail and, therefore, since the direction of the solar sail perturbation must be opposite to the direction of all perturbations, the incident angle cannot be controlled. The maximum area of the solar sail imposed were 500 m^2, but if this area could vary freely, the solar sail would be able to control all the perturbations for this case, since the incident angle is not larger than 90 degrees and there is no passage by the shadow of the Earth.

Figures 7 to 9 show the unit vector of the direction of the perturbations forces for the sum of the perturbations that act on the satellite and the direction of the solar radiation pressure caused by the solar sail.

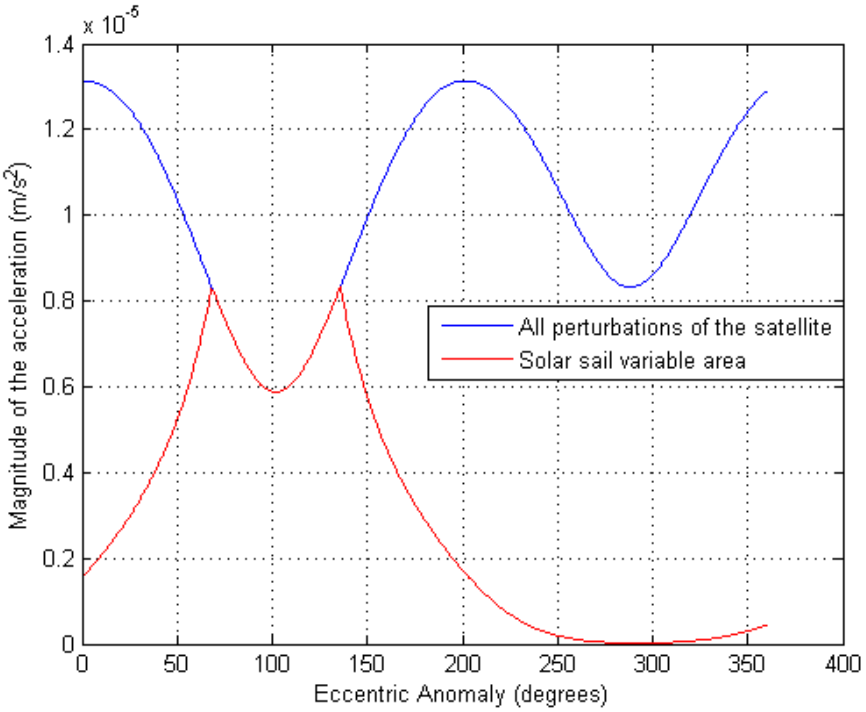

Figure 4. The magnitude of the acceleration VS. the eccentric anomaly of the spacecraft.

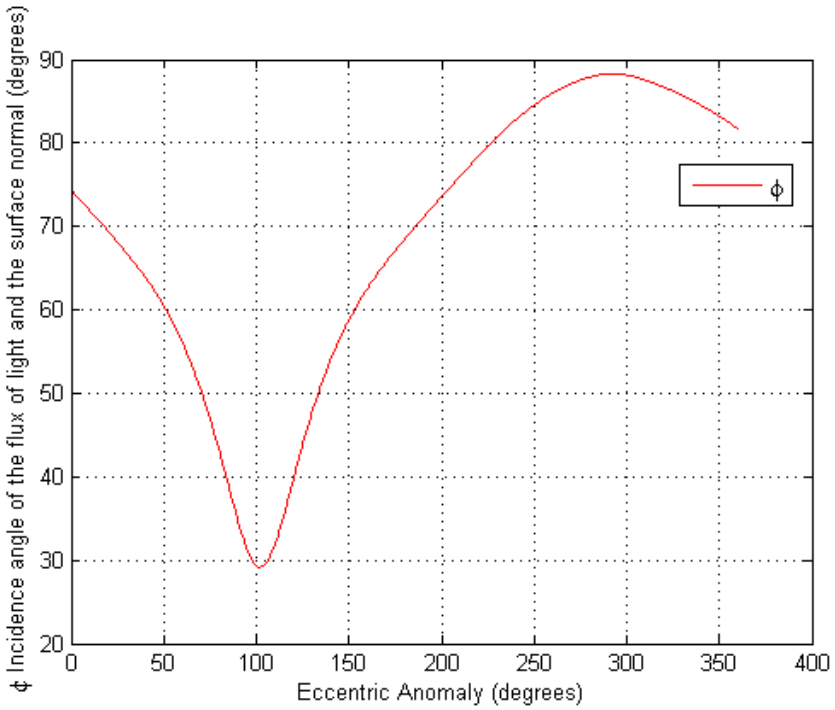

Figure 5. The incidence angle ∅ VS. the eccentric anomaly of the spacecraft.

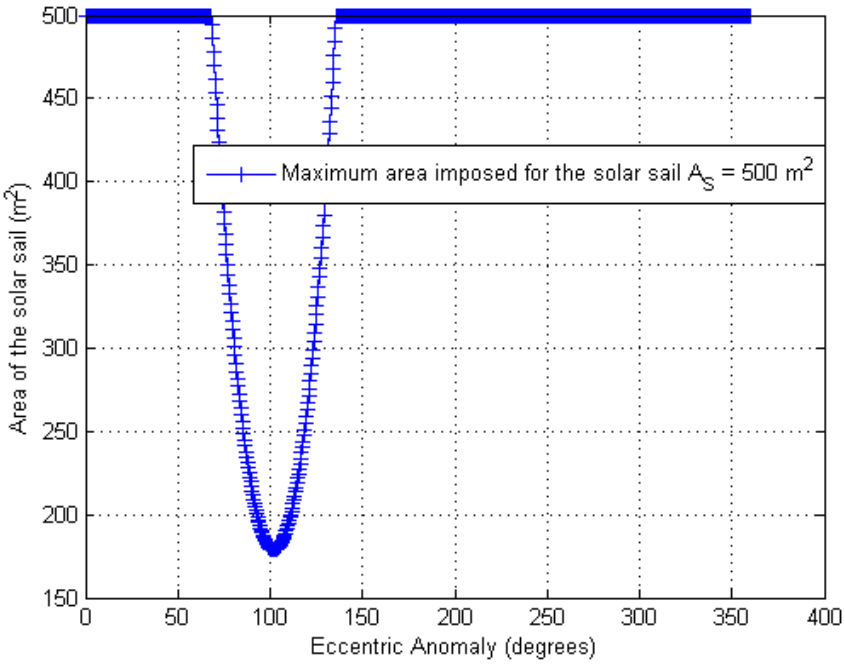

Figure 6. Maximum area of the solar sail VS. the eccentric anomaly of the spacecraft.

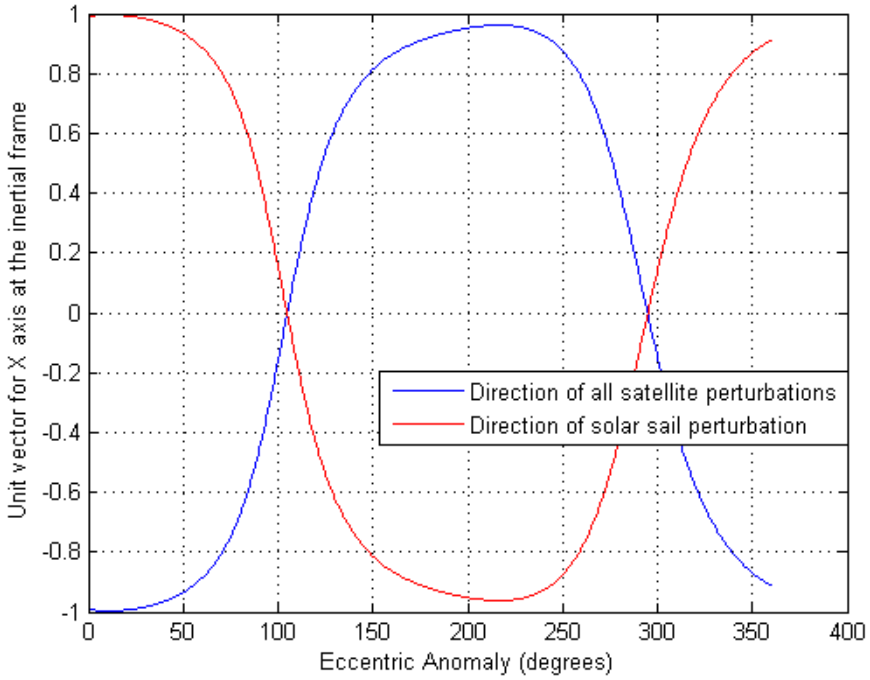

Figure 7. Unit vector for the X axis at the inertial frame VS. the eccentric anomaly of the spacecraft.

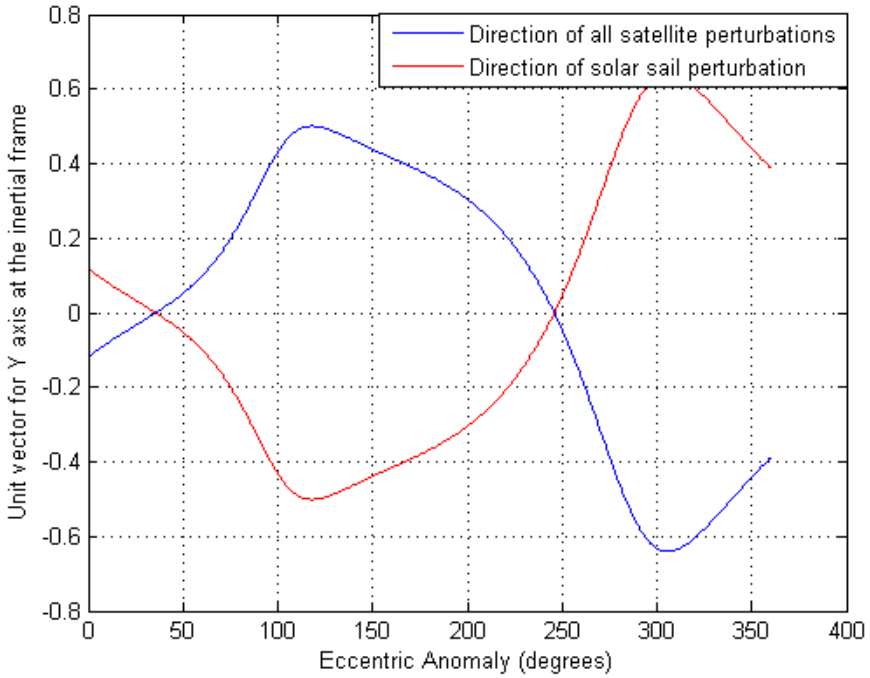

Figure 8. Unit vector for the Y axis at the inertial frame VS. the eccentric anomaly of the spacecraft.

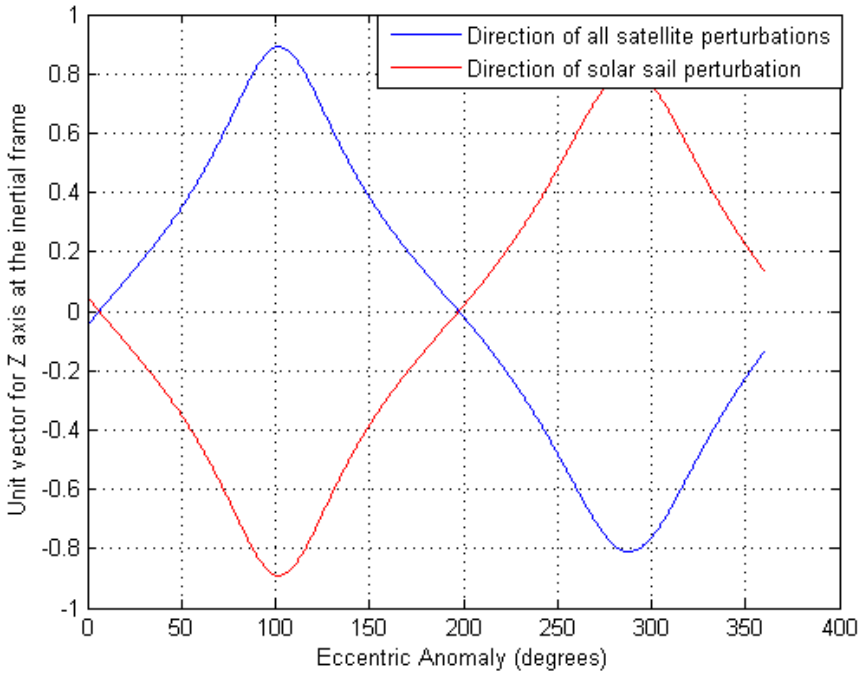

Figure 9. Unit vector for the Z axis at the inertial frame VS. the eccentric anomaly of the spacecraft.

From Figures 7 to 9, it is clear that the direction of the perturbations forces that act on the satellite is opposite to the direction of the solar radiation pressure caused by the solar sail. The opposite direction is required in order to guarantee that the perturbation forces are compensated or reduced.

As mentioned before, the solar sail is not always able to control or compensate totally the perturbation forces. If the incident angle is larger than 90 degrees, the solar sail perturbation caused by the solar radiation pressure is not able to compensate the perturbation forces or if the satellite has a passage through the shadow of the Earth. The second case for the optimal solution has those two different reasons for the inability of the solar sail to control or reduce the effects of the other perturbation effects and it is presented in Figures 10 to 12.

The second analysis for the optimal case begins the simulation in September 1, 2014 at 5:30 GMT. The results related to this case are shown in Figures 10 to 12.

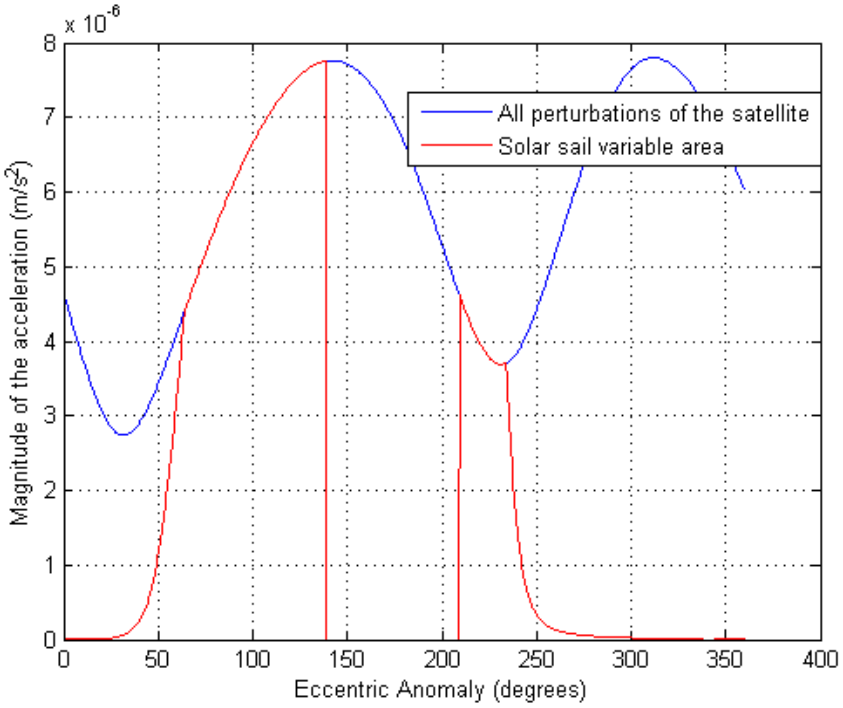

Figure 10. The PI value VS. the eccentric anomaly of the spacecraft.

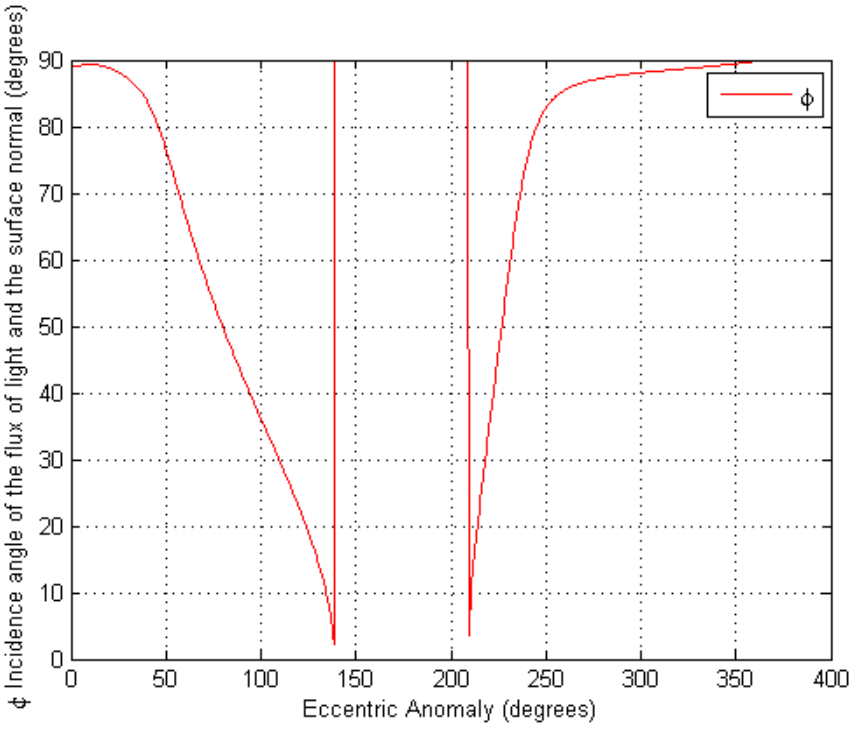

Figure 11. The incidence angle ∅ VS. the eccentric anomaly of the spacecraft.

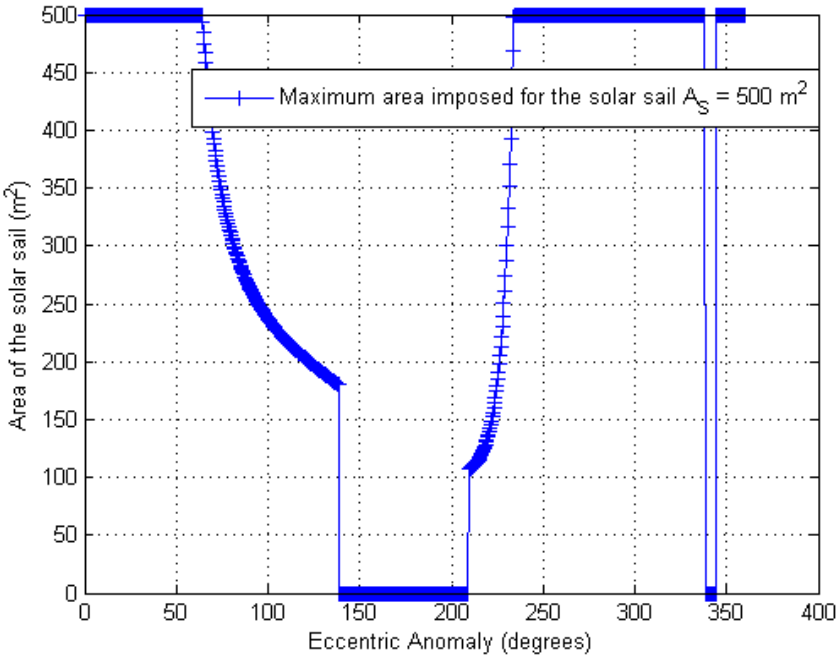

Figure 12. Maximum area of the solar sail VS. the eccentric anomaly of the spacecraft.

For this second case of the optimal solution for the solar sail, the range of the eccentric anomaly that the solar sail can control the other perturbation forces is different from the first case, shown in Figure 4.

From 338 to 345 degrees for the eccentric anomaly, the satellite passes through the shadow and the penumbra of the Earth.

Figure 11 provides the optimal incidence angle that the flux of the light of the Sun must have with the normal of the solar sail. From 140 to 210 degrees for the eccentric anomaly, the incidence angle is larger than 90 degrees, therefore, the default value of 90 degrees is considered for this range. If the incidence angle is larger than or equal 90 degrees, the solar sail cannot compensate the other perturbation forces since, for this geometry, it is not possible to obtain an opposite direction of the solar radiation pressure with the perturbation forces. Figure 11 does not consider the satellite passage through the shadow of the Earth, just the optimal angle of incidence.

In Figure 12 there is the optimal area of the solar sail with the maximum value restricted to 500 m^2. The area of the solar sail reduces to zero when the incidence angle is larger or equal 90 degrees or when the satellite passes thought the shadow of the Earth. The solar sail becomes inactive by rotating the panel of the solar sail in a way that the solar radiation pressure has no effect on the solar sail.

Sub-optimal Case with Fixed Area and Optimal Attitude for the Solar Sail

This sub-optimal approach considers now a fixed area for the solar sail, although the solar sail can have the optimal attitude to guarantee that the direction of the solar sail perturbation is opposite to the sum of all perturbations.

For the Figure 13, the area of the solar sail is now fixed and it is clear that the behavior for the magnitude of the acceleration is different from Figure 4. Now, the patterns of the magnitude of

the acceleration of the solar sail do not follow the patterns for all perturbations when they have the same magnitude and it occurs because the size of the solar sail is now fixed. Figures 8 to 10 are related to the direction of the solar sail perturbation in the optimal case is the same for this one, since the orbit and the initial conditions are the same, as well as Figure 5, with the optimal incidence angle for this case.

Sub-optimal case with Fixed Area and Constrained Attitude of the Solar Sail

This last sub-optimal case, with constraints not only in the fixed area of the solar sail, but also with constraints in the attitude of the solar sail, is exemplified in Figure 3. The analysis for this sub-optimal case begins the simulation in January 01, 2014 at 5:30 GMT (the same initial parameters for the first optimal case and for the first sub-optimal case).

For this case, some considerations must be explained before the results. Since the attitude of the solar sail is now constrained, the optimal direction of the attitude of the solar sail cannot be used in this case. Whenever the constrains do not allow the attitude of the satellite to be optimal, the attitude of the solar sail is given by the minimum deviation of the perturbation force caused by the solar sail constrained and the optimum solar sail. The constraint deviates the optimal direction of the solar sail, and when the angle between the optimal solution and the constrained solution for the solar sail force is larger than $\pi/2$, the solar sail constrained is disregarded and it becomes inactive.

Figure 14 shows the magnitude of the perturbations and the magnitude of the solar sail with the attitude constraint. This result is different from the one shown in Figure 13. The attitude constraints keep the satellite in a different attitude from the optimal result, and, by that, the incidence angle $\emptyset$ of the flux of energy of the Sun with the normal of the solar sail also changes. Figure 15 shows the incidence angle for the solar sail with attitude constraint.

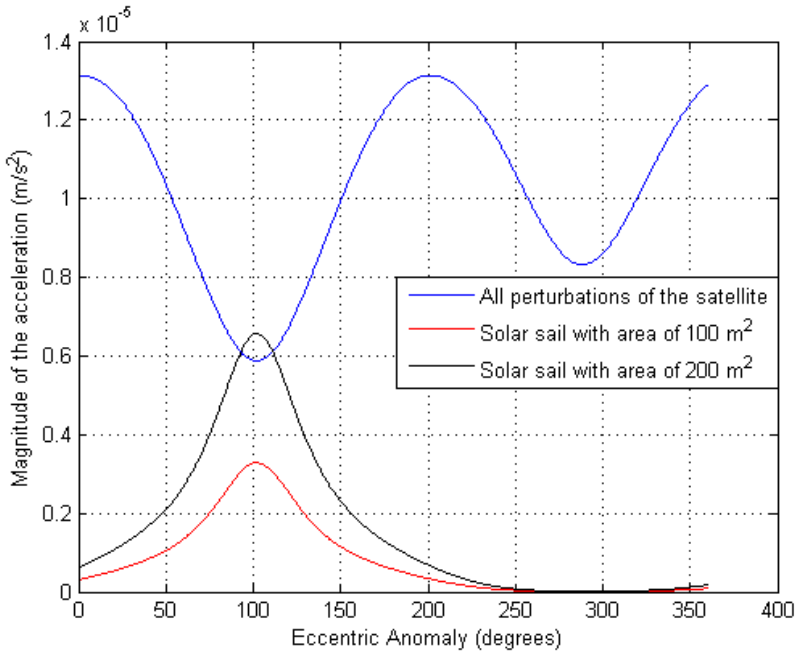

Figure 13. The magnitude of the acceleration VS. the eccentric anomaly of the spacecraft.

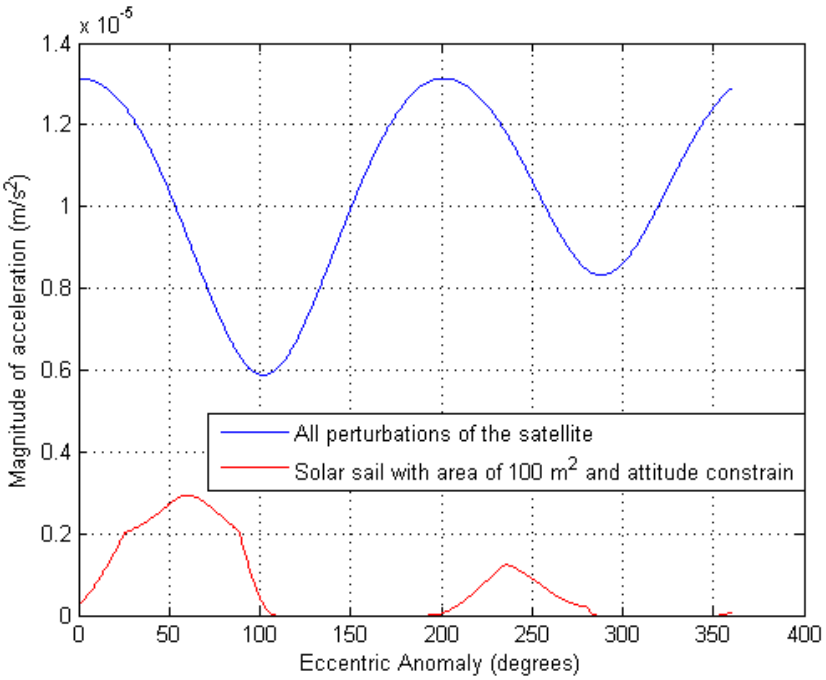

Figure 14. The magnitude of acceleration VS. the eccentric anomaly of the spacecraft.

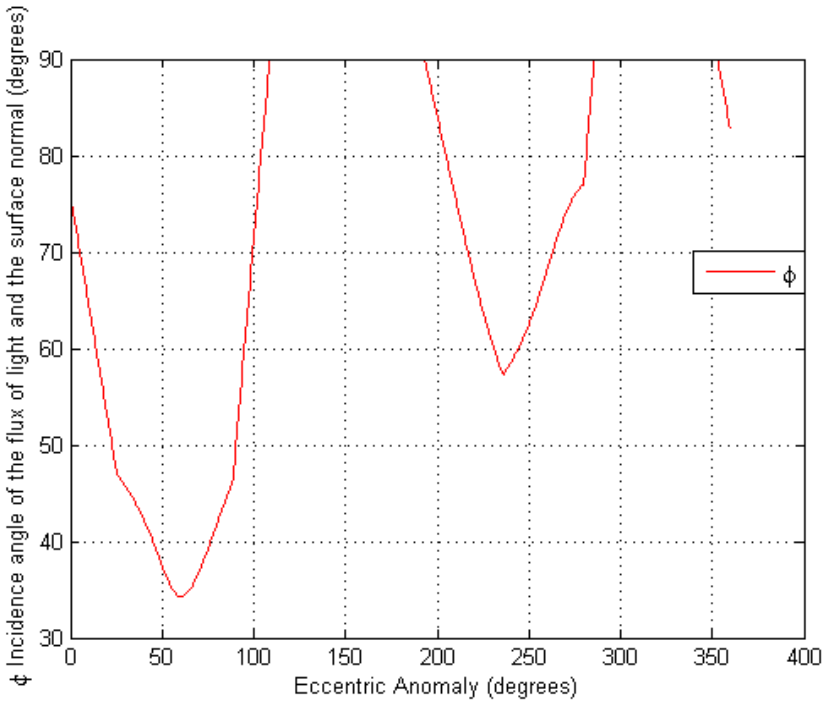

Figure 15. The incidence angle ∅ VS. the eccentric anomaly of the spacecraft.

The initial conditions of this case are the same ones of the first optimal result and of the first sub-optimal result. Figures 16 to 18 are related to the optimal and sub-optimal (constrained atti-

tude) direction of the normal of the satellite in the inertial frame. Those figures show the direction that the normal of the solar sail or the attitude that solar sail have for those three cases.

The blue line in Figures 16 to 18 represents the unit vector directions of the normal of the solar sail for the optimal direction with no constraint imposed for the attitude. The red line is related to the normal solar sail with the attitude constraint. The results are given in the inertial reference system fixed on the centre of the Earth and with the X axis pointed to the vernal point.

The results show the directions that the solar sail must have in order to compensate the other perturbation effects for the cases considered by creating a solar sail perturbation direction opposite or almost opposite to the other perturbations directions.

The Perturbation Integral Values

This section is related to the values of the perturbation integrals. As mentioned in the previous sections, the perturbation integral is used to evaluate the magnitude of the perturbations with and without the use of the solar sail. The results of this integral are important to evaluate how much the solar sail can compensate the magnitude of the perturbation forces. As shown in Table 2, there is a PI value for each different cases of the solar sail. The results are based on simulations that begin in January 01, 2014 at 5:30 GMT.

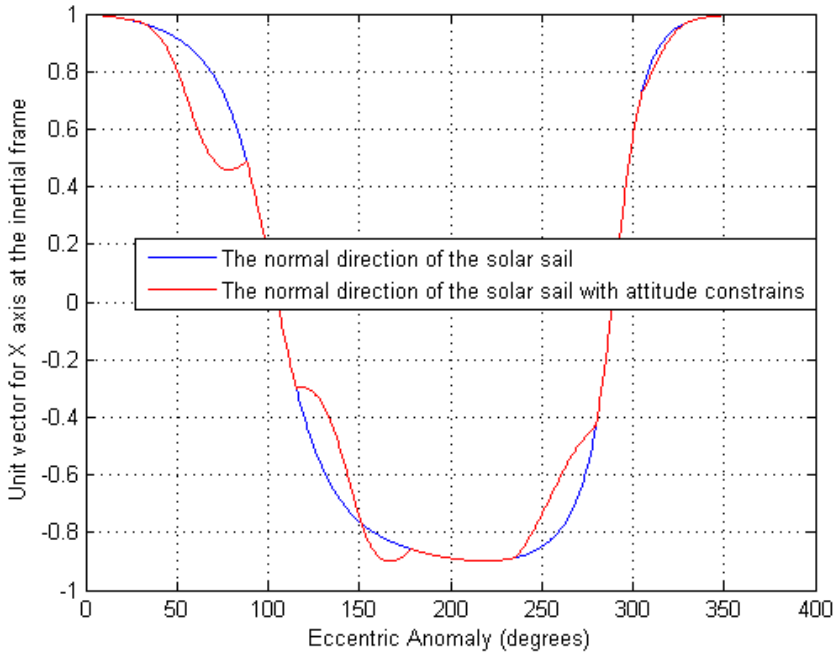

Figure 16. The normal unit vector direction for the X axis in the inertial frame VS. the eccentric anomaly of the spacecraft.

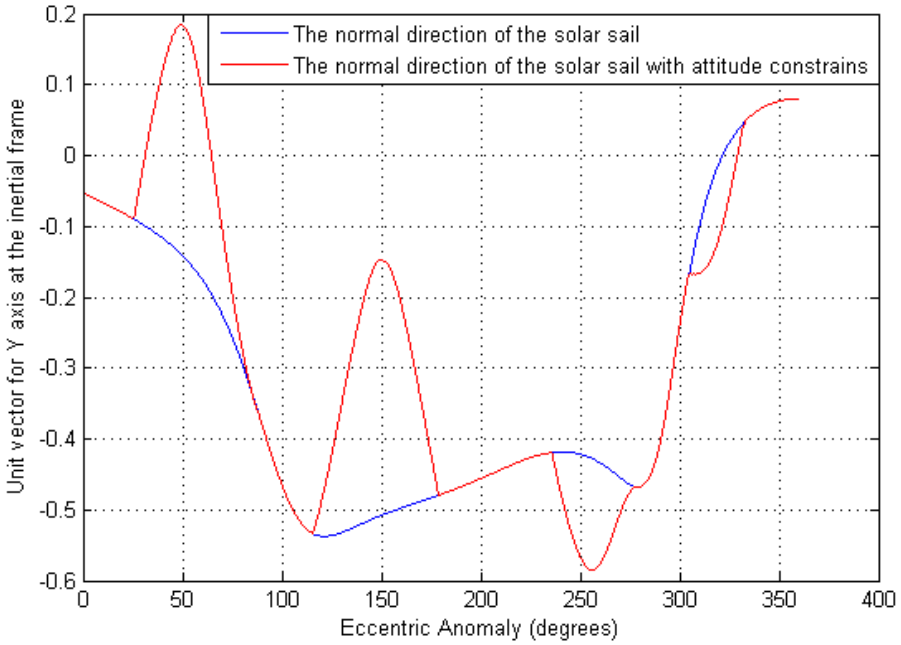

Figure 17. The normal unit vector direction for the Y axis in the inertial frame VS. the eccentric anomaly of the spacecraft.

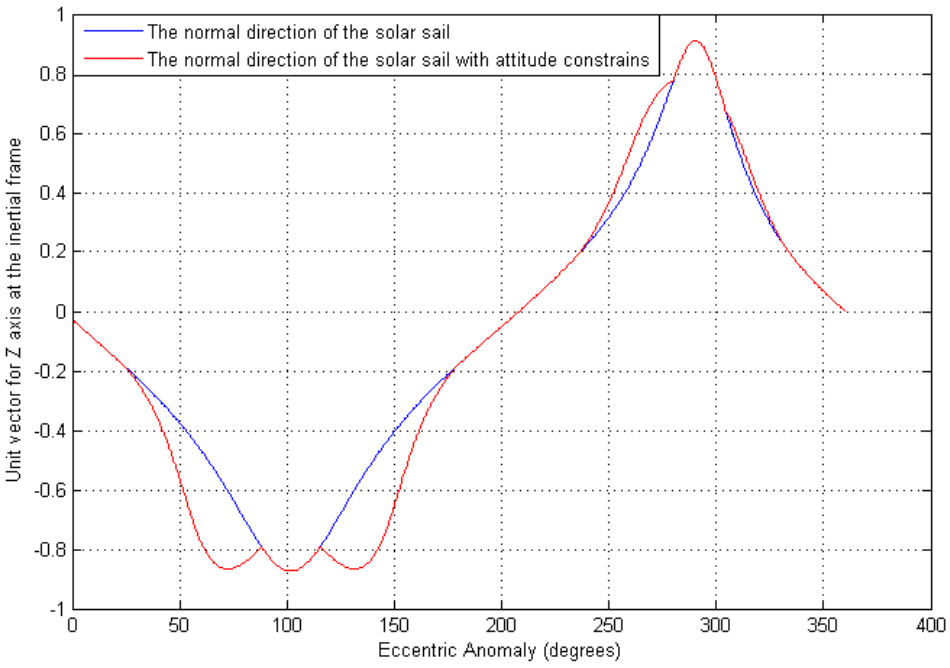

Figure 18. The normal unit vector direction for the Z axis in the inertial frame VS. the eccentric anomaly of the spacecraft.

Table 2. The PI values for the Geostationary Orbit based in Tables I and II.

	Solar Sail optimal with no area or attitude constraints	Solar sail sub-optimal with fixed area and no constraints for the attitude (100 m^2)	Solar sail sub-optimal with fixed area and no constraints for the attitude (200 m^2)	Solar sail sub-optimal with fixed area and attitude constraints
Jn Perturbation	0.5935 m/s	0.5935 m/s	0.5935 m/s	0.5935 m/s
Third-Body perturbation of the Moon	0.5993 m/s	0.5993 m/s	0.5993 m/s	0.5993 m/s
Third-body perturbation of the Sun	0.2236 m/s	0.2236 m/s	0.2236 m/s	0.2236 m/s
Solar radiation pressure of the satellite shape	0.0116 m/s	0.0116 m/s	0.0116 m/s	0.0116 m/s
Sum of all perturbations	0.8816 m/s	0.8816 m/s	0.8816 m/s	0.8816 m/s
Solar sail perturbation	0.2515 m/s	0.0699 m/s	0.1398 m/s	0.0588 m/s
All perturbations with the solar sail	0.6301 m/s	0.8117 m/s	0.7418 m/s	0.8228 m/s

From Table 2 it is possible to see that, for the optimal case, there is a reduction of 28,52% on the magnitude of the disturbing forces. For the sub-optimal solar sail with optimal attitude and fixed area of 100 m^2 the reduction is 7.63 % and for the fixed area of 200 m^2 the reduction is 15.85 %. The worst scenario, with fixed area and attitude constraints for the solar sail, the reduction on the magnitude of the disturbing forces is around 6.67%. For the optimal attitude of the solar sail, the PI value of all perturbations with the solar sail usage is actually the subtraction of the PI value of the sum of all perturbations with the PI value of the solar sail perturbation. This result occurs because the optimal attitude for the solar sail guarantees that the disturbing forces acting on the satellite and acting on the solar sail are opposite. Therefore, the constrained attitude of the solar sail does not have this result, since the direction of those forces are not opposite.

The other approach used in this paper was to keep the same initial parameters of the simulations of Table 2, but now varying the eccentricity of the orbit in Table 3 and the inclination in Table 4. Similar studies are made in the literature[1,2,3,19]. For the next Tables, only the sub-optimal case with area of the satellite fixed in 100 m^2 and the optimal attitude for the solar sail was considered.

Table 3. The Average Value of PI as the Eccentricity changes

	Sum of all perturbations	All perturbations with the solar sail usage	Percentage of reduction of the PI value with the solar sail
Eccentricity = 0	0.6370 m/s	0.5625 m/s	11.70%
Eccentricity = 0.2	0.7417 m/s	0.6545 m/s	11.76%
Eccentricity = 0.4	1.1226 m/s	1.0310 m/s	8.16%
Eccentricity = 0.6	2.2489 m/s	2.1644 m/s	3.76%

Table 4. The Average Value of PI as the Inclination changes

	Sum of all perturbations	All perturbations with the solar sail usage	Percentage of reduction of the PI value with the solar sail
Inclination = 0 grad	0.6370 m/s	0.5625 m/s	11.70%
Inclination = 20 grad	0.6516 m/s	0.5806 m/s	10.90%
Inclination = 40 grad	0.8143 m/s	0.7328 m/s	10.00%
Inclination = 60 grad	0.9256 m/s	0.8451 m/s	8.70%
Inclination = 80 grad	0.9257 m/s	0.8474 m/s	8.45%

From Tables 3 and 4, it is clear that when using the solar sail with fixed area but optimal attitude, the reduction of the PI value is almost the same, in absolute values, as the Keplerian elements vary, since the area of the solar sail is fixed. Nevertheless, the percentage of this reduction decreases as the sum of all perturbation increases. For all perturbations, as shown in some references, the sum of all perturbations increases as the inclination and eccentricity of the orbit increase (in the range shown), therefore these results were expected.[1,2,3]

CONCLUSION

This paper is concerned with the use of the solar radiation pressure perturbation of a solar sail to reduce the effects of the other perturbation forces along the orbit. The method used a given absorption factor for the solar sail material. The incidence angle that the flux of energy from the Sun makes with the normal of the satellite must be found to guarantee that the direction of the solar sail force is opposite to the sum of the other perturbations.

The solutions presented in this paper are optimal and sub-optimal in terms of the attitude of the solar sail. In particular, if the orbit must be keplerian all the time or if the tolerance of deviations parameters from the keplerian elements is small, the results are close to the PI values presented in this paper.

It is also important to point out that, if the tolerance deviation of the Keplerian elements of the orbit is high, the results showed here may have larger deviations from the fuel consumed, since

the proposed usage of the solar sail in this paper is to correct the deviations of the perturbation forces all the time.

The results have shown that the solar sail can be used to reduce the other disturbing forces and, therefore, decrease the fuel costs of the station keeping maneuvers.

REFERENCES

[1]Prado, A.F.B.A., "Searching for Orbits with the Minimum Fuel Consumption for Station-Keeping Maneuvers: Application to Luni-Solar Perturbations." Mathematical Problems in Engineering (Print), Volume 2013(2013), Article ID 415015, 11 pages.

[2] Oliveira,T.C.,Prado, A.F.B.A., Rocco, E. M. and Misra, A. K., "Searching for orbits that can be controlled by natural forces", AAS/AIAA Astrodynamics Specialist Conference, Hilton Head Island, South Carolina, 2013, paper 13-864, 20 pages.

[3] Oliveira,T.C.,Prado, A.F.B.A., Rocco, E. M., "Study of the Fuel Consumption for Station-Keeping Maneuvers for GEO satellites based on the Integral of the Perturbing Forces over Time" World Scientific and Engineering Academy and Society, Brasov, Romania, June 1-3, 2013.

[4]Anderson, J. D., "Fundamentals of Aerodynamics", 4th ed., New York, USA: McGraw Hill, 2007.

[5]Stuch, B. W., "Solar Pressure Three-Axis Attitude Control', Journal of Guidance, Control and Dynamics, Vol. 3, Issue no. 2, pp. 132-139, 1980.

[6]Polyaka, Y. N., "Solar Radiation Pressure and the Motion of Earth Satellites", AIAA Journal, Vol. I, Issue no. 12, pp. 2893-2909, December 1963.

[7]Williams, T. and Wang, Zhong-Sheng, "Potential Uses of Solar Radiation Pressure in Satellite Formation Flying", in AAS/AIAA Spaceflight Mechanics Meeting, Crearwater, Florida, 2000, AAS 00-204, pp.1599-1611.

[8]Dev Kumar, K., Bang, Hy-Choong, and Tahk, Min-Jea, "Formation Flying Using Solar Radiation Pressure", in 24th International Symposium on Space Technology and Science, Miyazaki, Japan, May 30-June6, 2004, ISTS 2004-d-25.

[9]Fieseler, P. D., "A method for Solar Sailing in a low Earth Orbit", ActaAstronautica, Vol. 43, No. 9-10, pp. 531-541, 1998.

[10]Capó-Lugo, P. A. and Bainum, P. M., "Orbital Mechanics and Formation Flying: A digital approach perspective", Woodhead publishing in mechanical engineering, ISBN: 978-0-85709-054-6.

[11]Longo, C. R. O. and Rickman, S. L., "Method for the Calculation of the Spacecraft Umbra and Penumbra Shadow Terminatior Points", NASA Technical Paper 3547.

[12]Borgraafe, A., Heiligers, J., Ceriotti, M., McInnes, C., " Optical Control of Solar Sails using Distributed Reflectivity", Spacecraft Structures Conference, Chapter DOI: 10.2514/6.2014-0833,13-17 January 2014.

[13]Simpson, David G. (1999).An Alternative Lunar Ephemeris Model for On-Board Flight Software Use.In *Procedings of the 1999 Flight Mechanics Symposium* (ed. John P. Lynch), NASA Goddard Space Flight Center, pp. 175-184.NASA Publ. NASA/CP-1999-209235.

[14]Michalsky, J. J. "The Astronomical Almanac's Algorithm for Approximate Solar Position (1950-2050)".Solar Energy.Vol. 40, No. 3, 1988; pp. 227-235, USA.

[15]Carrara, V. PROPAT – Satellite Attitude and Orbit Tootlbox for Matlab, online: http://www2.dem.inpe.br/val/projetos/propat/default.htm.

[16]Kuga, H. K.; Carrara, V.; Rao, K. R. Satélites Artificiais - Movimento Orbital. São José dos Campos: INPE, 2011. 103 p. (sid.inpe.br/mtc-m19/2011/11.22.18.25-PUD).

[17]Tewari, A.,"Atmospheric and space flight dynamics modeling and simulation with Matlab and Simulink", Boston, MA : Birkhauser, 2007. 556 p. ISBN 978-0-817-64373-7

[18]Oliveira,T.C., Prado, A.F.B.A. and Misra, A. K., "Determining orbits that can be controlled by natural forces", 24th AAS/AIAA Space Flight Mechanics Meeting, Santa Fe, New Mexico, January 26-30, 2014., paper 14-426, 20 pages.

[19]Prado, A.F.B.A., "Mapping Orbits Around the Asteroid 2001SN263".Advances in Space Research. Vol. 53, 2014; pp. 877-889.